

# DETAILED RESEARCH ON RICH-LEAN TYPE SINGLE SECTOR AND FULL ANNULAR COMBUSTOR FOR SMALL AIRCRAFT ENGINE

Mitsumasa MAKIDA, Hideshi YAMADA and Kazuo SHIMODAIRA\*  
\* Japan Aerospace Exploration Agency

## Abstract

*In the TechCLEAN project of JAXA, experimental research has been conducted to develop a combustor for a small aircraft engine. The combustor was tuned to show the behavior of the Rich-Lean combustion through tests under atmospheric and practical conditions. Finally, through full annular combustion experiment under practical conditions, the combustor was tuned to reduce NO<sub>x</sub> emissions to 38% of the ICAO CAEP4 standard, also sustaining low CO and THC emissions. Successively, to investigate the performance of the combustor in detail, parametric experiments were conducted with single-sector and full annular combustors under additional test conditions with inlet air temperature from 450K to 700K. Furthermore, detailed measurements at the full annular combustor exit were also conducted to obtain the distribution of temperature, pressure and gas composition, using a traversable measuring system. The correlation between measured emissions data and test conditions are estimated to obtain the combustion characteristics of the rich-lean type combustor.*

## 1 Introduction

In general, small and medium power aircraft engines must simultaneously satisfy several requirements, for example, high efficiency, environmental friendliness and cost effectiveness [1]. From 2003 to 2012, Japan Aerospace Exploration Agency (JAXA) conducted a project "Technology development project for clean engines" (so-called TechCLEAN project), in which researches to

develop advanced combustion technology had been conducted aiming to reduce toxic exhaust gas compositions, especially NO<sub>x</sub>, from aeroengine combustors. And in the framework of the TechCLEAN project, JAXA had been developing aeroengine combustors for an affordable and environment-friendly small aircraft (with approximately 50-passengers). The designed thrust of the engine is about 40kN and the pressure ratio is about 20. The target of the combustor development is to reduce NO<sub>x</sub> emissions lower than 50% of the ICAO CAEP4 standard, aiming to go below the trend of reducing NO<sub>x</sub> emissions. Also aiming to reduce CO and THC emissions to 90% of the previous standards and ensure basic performance of aero engine combustors, such as ignition and blowout.

The overview of the development process of our combustor is shown in Fig.1 with Technology Readiness Level (TRL). We started from preliminary combustion tests with tubular combustors under atmospheric conditions. Then both model combustors and test conditions got closer to the target engine combustor step by step, and finally full annular combustors were tested under practical conditions and succeeded to reduce NO<sub>x</sub> emissions to 38.1% of the ICAO CAEP4 standard, which are shown in the lower right of Fig.1, also reducing CO, THC and smoke emissions [2-6].

Besides, during the development process under practical conditions, combustion tests were only conducted under ICAO Landing and Take-Off (LTO) cycle conditions of the target engine, whose numerical value could not be presented in detail. So in this report, in order to obtain and report more detailed data which can be utilized for further combustor improvement,

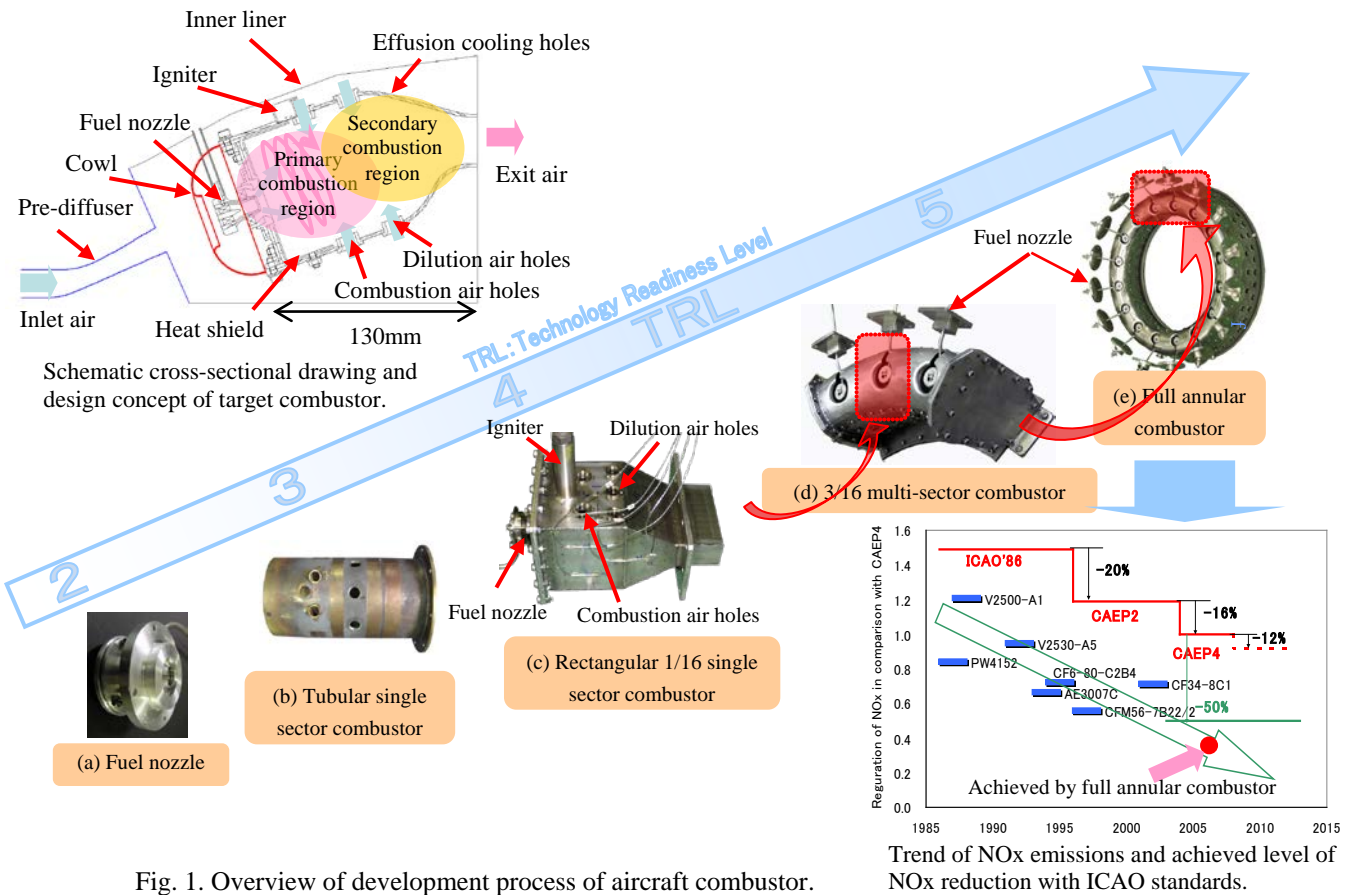


Fig. 1. Overview of development process of aircraft combustor.

we conducted combustion tests under parametric conditions with single-sector and full annular combustors under inlet air temperature increasing from 450K to 700K at 50K intervals. Also inlet pressure and mass flow rate of inlet air were increased in accordance with inlet temperature along the design line of ordinary small engines. For the full annular combustor, we have already reported results of combustion tests under parametric conditions up to 650K in the previous report [6]. In this report, we extended the temperature range to 700K, and we also conducted traverse measurements at the combustor exit in more detail.

Here, we start from the review of our previous reports and then present the procedure and results of parametric combustion tests of single-sector and full annular combustors.

## 2 Design Concept of Combustor

The development process of our combustor shown in Fig.1 was already discussed in previous reports [2-6]. But to make a smooth introduction to this report, some discussions

related to the design concept of the combustor are presented here. The upper left figure of Fig.1 shows a cross-sectional drawing of our combustor with descriptions explaining the preliminary design concept. Since one of the targets of this engine is to reduce the direct operating cost (DOC), the engine should be lightweight and simply structured. So the combustor is confined into a small space, and its fuel supply system is required to be simple. At the same time, the reduction of NOx emissions is also required, sustaining high combustion efficiency over a wide range of operating conditions [7]. For the target engine, the overall equivalence ratio of the combustor varies from 0.10 (idle condition) to 0.35 (full load condition). To satisfy these requirements simultaneously, the Rich-Lean combustion approach [8] was utilized for this combustor, and we applied the concept of single fuel supplied air blast type nozzle proposed by Parker-Hannifin [9], as shown in Fig.1a.

In the combustor concept mentioned above, two factors should play significant roles; the enhanced mixing in the primary combustion

Table 1. Inlet air conditions of parametric combustion tests. (Mass flow rate is for single-sector combustor, G:Gas sampling, T:Traverse, X:Not measured.)

Temperature $T_{in}$ (K)	Pressure (MPa)	Mass flow rate (kg/s)	AFR	Combustor	
				Sin.	Ann.
450	0.315	0.260	95.3	G	T, G
500	0.504	0.402	84.3	G	G
550	0.738	0.554	73.2	G	T, G
600	1,018	0.715	62.1	X	G
650	1,345	0.886	51.0	G	T, G
700	1,757	1.067	48.8	G	G

region, and the tuning of the air mass flow ratio among the fuel nozzle, the primary and secondary combustion regions and the wall cooling. A lot of research has been done on these factors [10-16], and also in our research, a large portion of effort has been concentrated on them.

### 3 Parametric Combustion Tests

#### 3.1 Parametric Tests Conditions

In the combustor development process mentioned above, the model combustors were tested under the ICAO LTO cycle conditions of the target engine up to 100%MTO, with inlet air temperature  $T_{in}$  up to around 700K and with inlet pressure up to 1.65MPa. In this report, in order to obtain more detailed data, we conducted parametric combustion tests of a rectangular single-sector and a full annular combustor with  $T_{in}$  increases from 450K to 700K at intervals of 50K. Also inlet pressure, air mass flow rate and air to fuel ratio (AFR) were changed along the design line of the target engine, as shown in Table 1. Here, the mass flow rate is for the single-sector combustor, that is, 1/16 of the full annular combustor. Symbols in the two right columns of Table 1 show measurement state as follows; gas sampling analysis for various AFR was conducted under conditions with "G", circumferential traverse measurements of temperature, pressure and gas compositions at the exit of the full annular combustor were conducted under conditions with "T", and no measurement was conducted under the condition with "X".

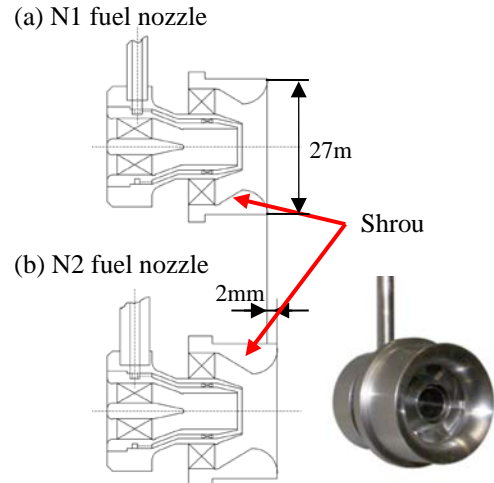


Fig. 2. Difference between N1 and N2 fuel nozzles.

Besides, we also applied slightly different types of fuel nozzle for the single-sector and the full annular combustors. Two types of fuel nozzles are shown in Fig.2; (a) the original type N1 and (b) modified type N2. The shroud of N2 was extended by 2mm aiming to improve fuel atomization. In the development process of the combustor, we applied N1. Then in the full annular combustion tests conducted in the previous report [6], both N1 and N2 nozzles were tested simultaneously, and N2 showed better combustion characteristics. So, we applied N1 to the single-sector combustor and N2 to the full annular combustor in this report.

#### 3.2 Setup of Single-Sector Combustor Tests

Under the parametric condition, the combustion tests were repeated under high temperature and pressure conditions. So the rectangular single-sector combustor was modified to the heat-resisting configuration as shown in Fig.3. Upper and lower liner walls and heat shields were made of hastelloy, and two sidewalls with effusion cooling air holes were replaced with adiabatic walls stuffed with heat insulating material. The cooling air holes on the sidewalls were moved to combustor liners, keeping the total effective area of cooling air holes. This means that the cooling of combustor liners was also enhanced.

The single-sector combustor was set into a high pressure combustion test casing as shown in Fig.4, and embedded in the "High-Temperature and Pressure Combustion Test

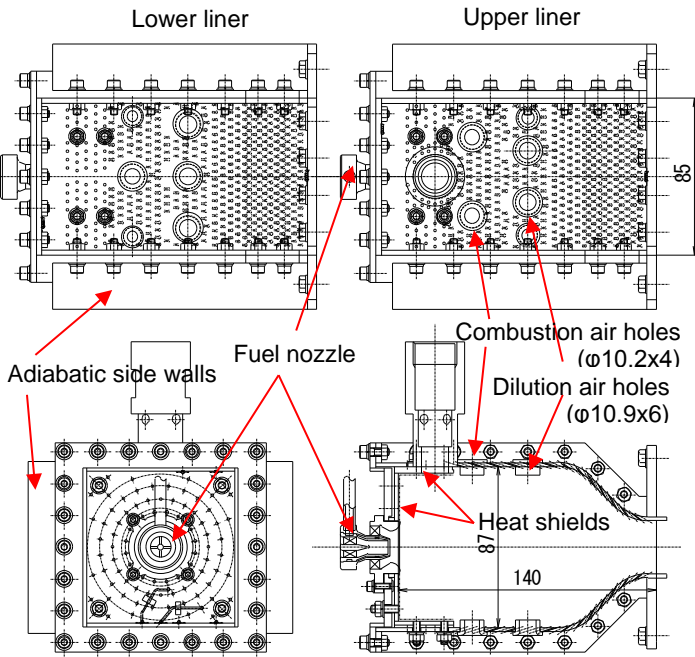


Fig. 3. Schematic drawings of rectangular single-sector combustor.

Facility" in JAXA. At this facility, compressed and electrically heated air was continuously supplied to the combustion test casing, and kerosene was used for the fuel. Test conditions were set as shown in Table 1.

Under these test conditions, exhaust gas composition and pressure at the combustor exit were measured by a nine-point collective hot-water-cooled sampling probe, located just below the combustor exit as shown in Fig.4. The sampled gas was led through the heated sampling line to the gas-analyzer "HORIBA MEXA-7100D" which measured the compositions of CO, CO<sub>2</sub>, THC (as CH<sub>4</sub>), NO, and NO<sub>x</sub> by generally used gas analysis procedures: chemiluminescence for NO,

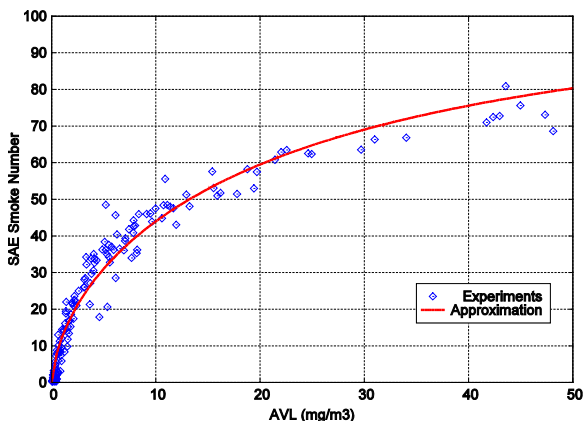


Fig. 5. Correlation of measured soot value between AVL (mg/m<sup>3</sup>) and SAE smoke number.

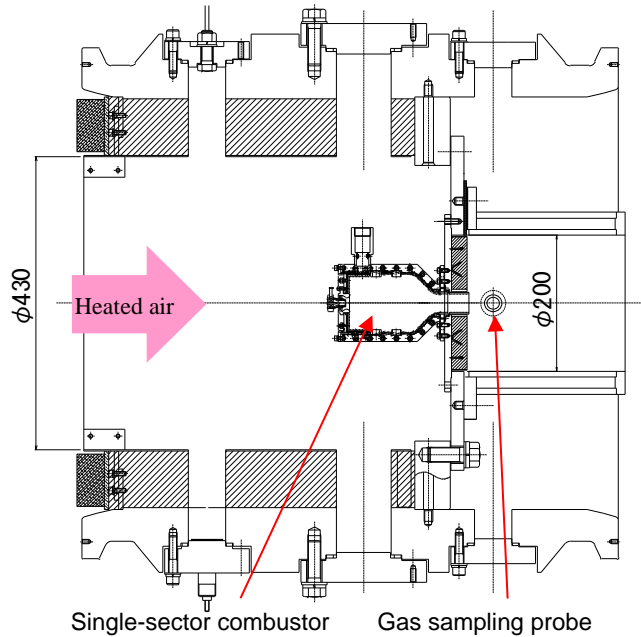


Fig. 4. Cross-sectional drawing of setup of rectangular single-sector combustor inside high-pressure combustion test casing.

nondispersive infrared absorption for CO and CO<sub>2</sub>, flame ionization for THC, and paramagnetic analysis for O<sub>2</sub>. These gas sampling procedures were based on the standard of the ICAO [17]. Pressure drops through combustors were estimated between a pressure probe in the upstream of the test casing and the sampling probe in the downstream of the combustor exit.

Meanwhile, the soot emission was mainly measured by a variable sampling smoke meter "AVL 415S", and for the calibration, soot was also measured by a smoke meter which was developed in JAXA in accordance with the SAE standard [18]. The soot emission measured by "AVL 415S" in the unit of mg/m<sup>3</sup> can be converted to SAE smoke number through the plots shown in Fig.5, which has been obtained through other combustion tests under high temperature and pressure conditions.

### 3.3 Setup of Full Annular Combustor Tests

Combustion tests of the full annular combustor were also conducted under parametric conditions at the "High-Temperature and Pressure Full Annular Combustor Test Facility" which was developed by JAXA in 2007. In Fig.6, a schematic drawing of the cross-section of the test facility near the full annular

**DETAILED RESEARCH ON RICH-LEAN TYPE SINGLE SECTOR AND FULL ANNULAR COMBUSTOR FOR SMALL AIRCRAFT ENGINE**

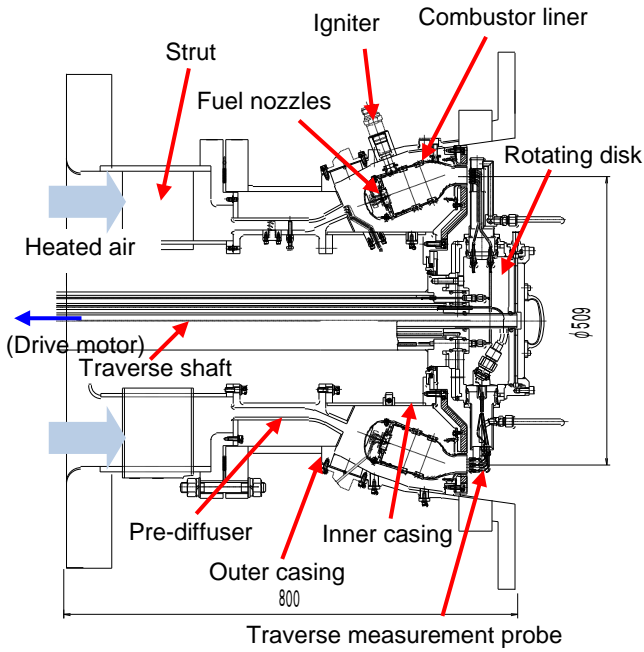


Fig. 6. Cross-sectional drawing of combustion test section (including traverse measurement system).

combustor is shown. Jet-A1 was used for the fuel. The detail of this facility was already introduced in the previous reports [4-6], but some specifications related to measurements in this report are mentioned here again.

In addition to the emission characteristics, the temperature distribution at the combustor exit is also one of the very important performances, required from the design of turbine blades, which are located in the downstream of combustors. Therefore, detailed measurement has been conducted for the exit temperature, pressure and gas composition distributions. So far, these exit properties were measured by fixed rakes or probes, thus the number of sampling point were very limited. Our test facility has a traversable measuring system in the downstream of the combustor exit as shown in Fig.6, and it enabled detailed traverse measurement of the exit temperature, pressure and gas composition over 360 degrees.

The detail of the traverse measurement system is shown in the upper figure of Fig.7, which is seen from the downstream of the combustor exit. Exit temperature is measured by two temperature sensor rakes Te1 and Te2, and exhaust gas composition and pressure are measured by two five-point probes Dp1 and Dp2. Each rake and probe has five sampling

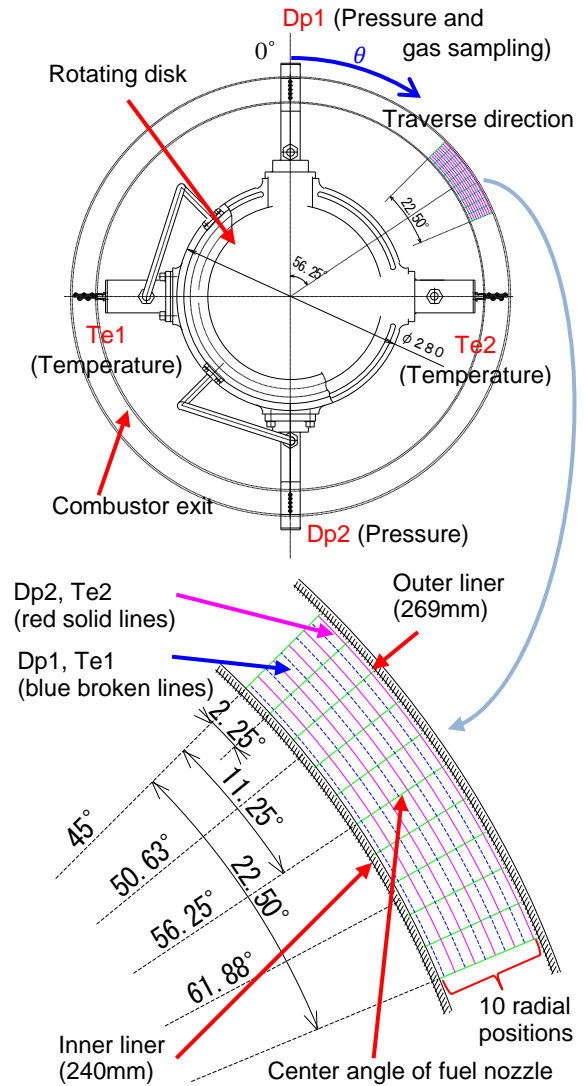


Fig. 7. Backsight of traverse measurement system and example of sampling points.

points in the radial direction as shown in Fig.8. Each pair of rake and probe is mounted axial symmetry with 180 degrees on the rotating disk. As shown in Fig.6, the rotating disk is connected to the drive motor with the long traverse shaft passing through the combustion test section. It can rotate within a range of  $\pm 185$  degrees and has the feedback control with the accuracy of 0.5 degrees. The rotating disk, the rakes and probes are cooled by the pressurized hot water provided through the traverse shaft. The sampled gas from the five-point probe Dp1 is led through the shaft, being kept warm with pressurized hot water (3MPa, 430K), then collected to one line and led to the gas analyzers through a heated sampling line. Then the sampled gas was analyzed by the same

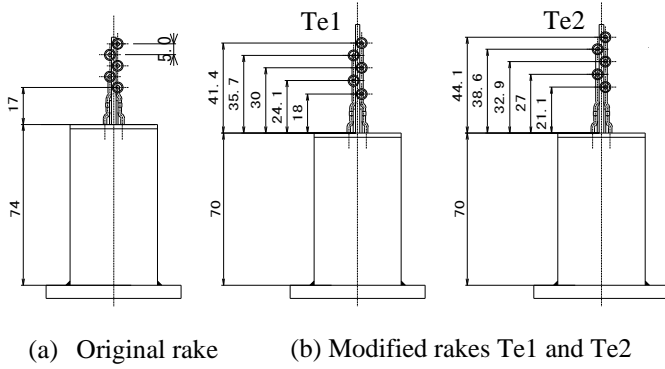


Fig. 8. Comparison between original and modified temperature sensor rakes.

procedure as mentioned in the previous section for the single-sector combustor.

The traverse angle  $\theta$  was defined by the position of the probe Dp1. It started from 0 degrees, traversed in the clockwise direction (as shown by the blue arc arrow in Fig.7) at intervals of 2.25 degrees. On the other hand, the rakes Te1, Te2 and the probe Dp2 started from 270, 90 and 180 degrees respectively.

In the previous reports [4-6], five sampling points of each rake and probe were equally-spaced at intervals of 5mm in the radial direction as shown in Fig.8a, that is, they measured at the same radial positions. This means that the data of Te1 and Te2 obtained at the same angular position was measured with the interval of traverse for 180 degrees, which took about 25 minutes in detailed measurements. And from the results of the previous report [6], Te1 and Te2 showed close values, which means that the combustion was in a stable state. So in this report, we made an attempt to increase the sampling resolution in the radial direction to 10 points by shifting the radial position of sampling points as shown in Fig.8b and Table 2. Each sampling point was located to even out its covering area. In the lower figure of Fig.7, an example of measuring area is shown over the range of 22.5 degrees in the downstream of the fuel nozzle which is located at 53.25 degrees. The radial position of Te1 and Dp1 is shown by blue broken lines, and that of Te2 and Dp2 is shown by red solid lines. Then the sampling resolution becomes 10 points for both radial and circumferential directions, and totally 100 measuring points for each fuel nozzle, thus 1600 points for 360 degrees measurement.

Table 2. Radial sampling position of modified temperature rakes and pressure probes (mm).

Te1, Dp1			Te2, Dp2		
Position	Temp.	Press.	Position	Temp.	Press.
264.9	Te11	Dp11	267.6	Te21	Dp21
259.2	Te12	Dp12	262.1	Te22	Dp22
253.5	Te13	Dp13	256.4	Te23	Dp23
247.6	Te14	Dp14	250.5	Te24	Dp24
241.5	Te15	Dp15	244.6	Te25	Dp25

#### 4 Emission Characteristics of Single-sector and Full Annular Combustors

Exhaust gas was sampled and its composition was analyzed for both combustor models under parametric conditions, decreasing AFR from 160 to 30. For the single-sector combustor, the exhaust gas was measured by the nine-point collective sampling probe fixed just below the combustor exit. On the other hand, for the full annular combustor, the exhaust gas was measured by five-point sampling probe Dp1 fixed in the downstream of the fuel nozzle located at 56.25 degrees.

Emission results of both combustor models under each  $T_{in}$  condition are shown in Fig.9, 10 and 11. NO<sub>x</sub> emissions and combustion efficiency, and soot emission are plotted versus AFR in Fig.9 and 11 respectively. In addition, correlation of CO emission with NO<sub>x</sub> emissions is also shown in Fig.10. In these graphs, emissions of NO<sub>x</sub> and CO are expressed by emission index (EI), that is, grams of emitted matter per 1kg fuel. The combustion efficiency is calculated from the analyzed gas composition. Pressure drop through the combustor was observed between 3 and 4.5%. For this pressure drop, Sauter Mean Diameter (SMD) of the spray of this fuel nozzle was about 40 $\mu$ m, obtained from spray measurement under atmospheric pressure, while the diameter is expected to be smaller under high pressure conditions.

From Fig.9, we can see the Rich-Lean combustion behavior for both combustor models, that is, reduces NO<sub>x</sub> emissions at low AFR range, also sustaining high combustion efficiency. We can also see that EINO<sub>x</sub> plots have a common tendency under each  $T_{in}$  condition. By decreasing AFR from higher range, plots of EINO<sub>x</sub> have maximum values, then decrease, have minimum values in the AFR

**DETAILED RESEARCH ON RICH-LEAN TYPE SINGLE SECTOR AND FULL ANNULAR COMBUSTOR FOR SMALL AIRCRAFT ENGINE**

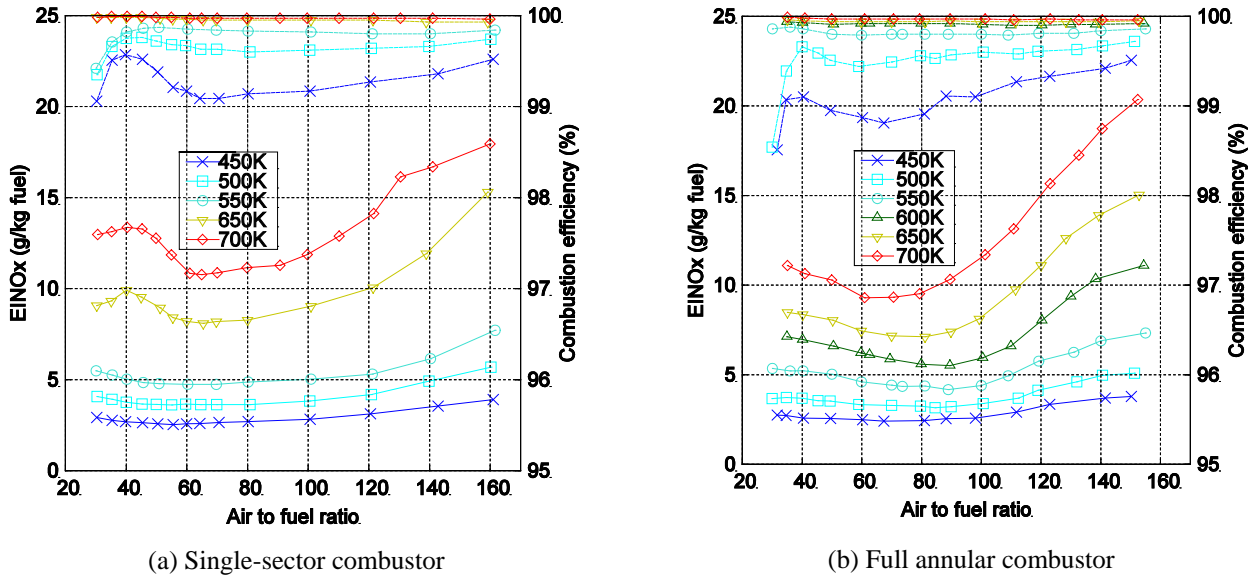


Fig. 9. NO<sub>x</sub> emissions and combustion efficiency versus air to fuel ratio under parametric conditions. (Solid lines: EINO<sub>x</sub>, broken lines: combustion efficiency).

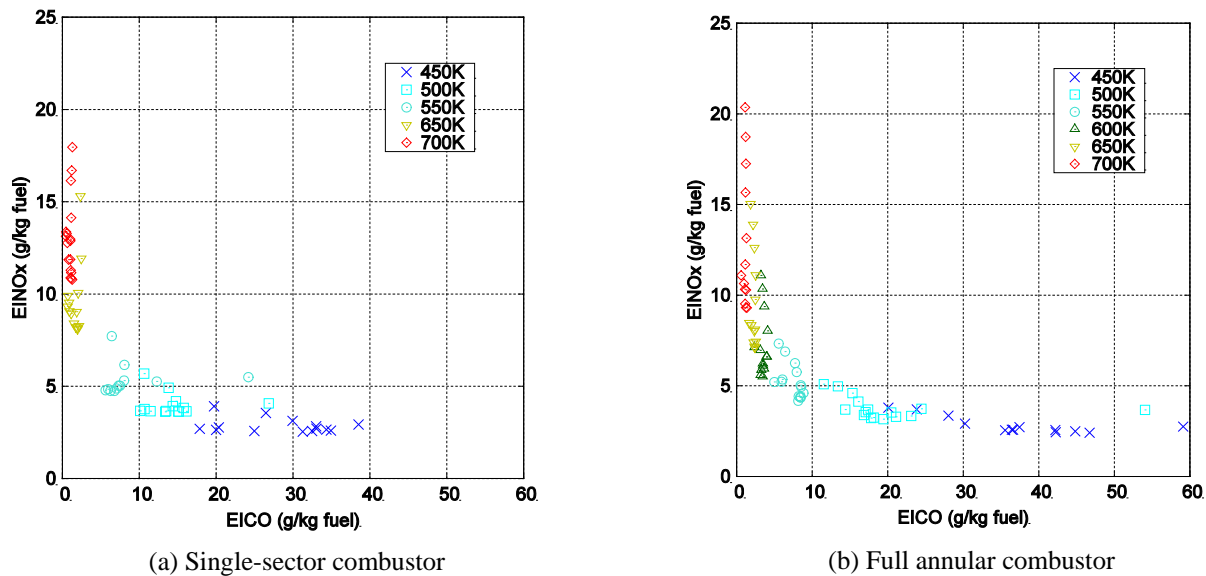


Fig. 10. Correlation of CO and NO<sub>x</sub> emissions under parametric conditions.

range between 60 and 100, and increase again in lower AFR range. Comparing combustor models (a) and (b) in Fig.9, combustion efficiency was lower for the full annular combustor, and consequently NO<sub>x</sub> emissions were also lower. But they show the same characteristics as mentioned above.

Besides, from emission correlations of CO with NO<sub>x</sub> shown in Fig.10, we can see that, for both combustor models, even the plot region shifts with  $T_{in}$ , CO and NO<sub>x</sub> emissions have a strong inverse correlation and there is no stray point. This means that oxidant and evaporated

fuel was sufficiently mixed and reacted for a whole AFR range of these combustion tests.

For the soot emission, as mentioned before, measured data by “AVL 415S” was converted to SAE smoke number through the plots shown in Fig.5. Converted plots in Fig.11 have peak values in the low AFR range between 50 and 70, and then decrease again in lower AFR range. As inlet temperature  $T_{in}$  (and also pressure) increases, soot emission got higher. As an exception, for the full annular combustor, the peak value of 650K is lower than that of 600K. Comparing (a) and (b) in Fig.11, they show the same emission tendency as mentioned before,

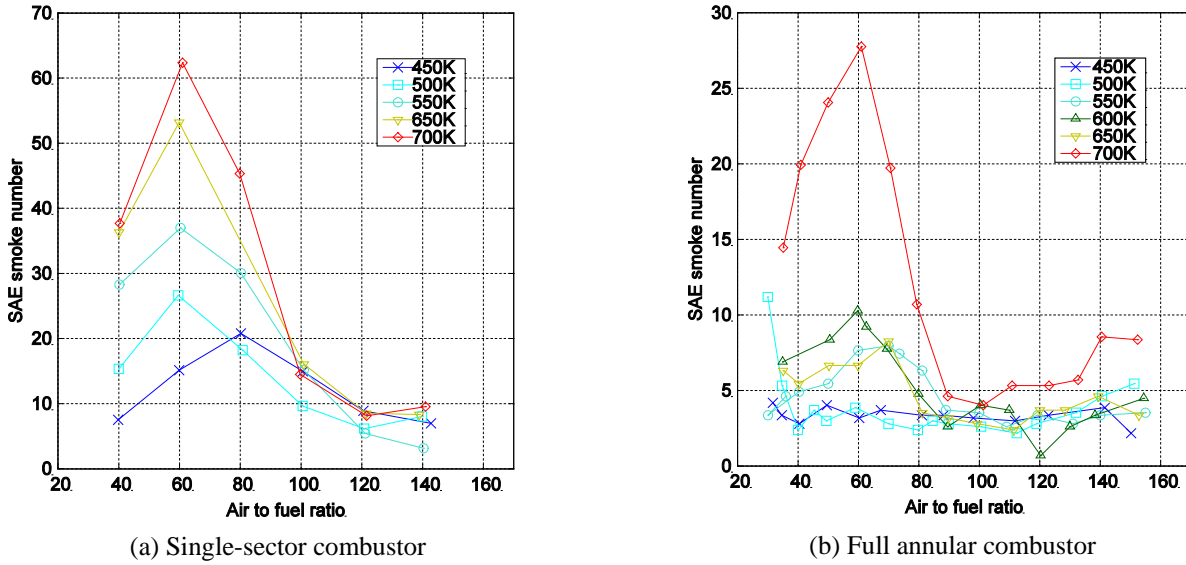


Fig. 11. Soot emission versus air to fuel ratio under parametric conditions.

but smoke number of the single-sector combustor was almost double of that of the full annular combustor. It must be caused by the difference of combustor configuration; rectangular or annular, especially by the existence of the adiabatic sidewalls of the single-sector combustor as shown in Fig.3.

### 5 Exit Temperature Distribution of Full Annular Combustor

For the annular combustor, we also conducted detailed traverse measurements at the combustor exit under  $T_{in}$  conditions of 450K, 550K and 650K. During the traverse measurements, AFR was fixed to the value shown in Table 1, and the rakes and probes were rotated at intervals of

2.25 degrees, that is, sampled at 160 points in the circumferential direction. As the gas compositions were also measured, it took about 50 minutes for a set of 360 degree measurement.

Figure 12 shows the circumferential exit temperature distribution measured by the temperature sensor rakes and averaged over the five points in the radial direction for both Te1 and Te2. Along with the horizontal axis, 16 fuel nozzles are allocated, started from 11.25 degrees at intervals of 22.5 degrees. Under  $T_{in}$  of 450K and 550K, each profile has clear shapes corresponding to the position of the fuel nozzles, and has peak value between each fuel nozzle. In these cases, profiles said to be stable, that is, kept during the traverse measurements for Te1 and Te2. But as  $T_{in}$  got higher to 650K, the

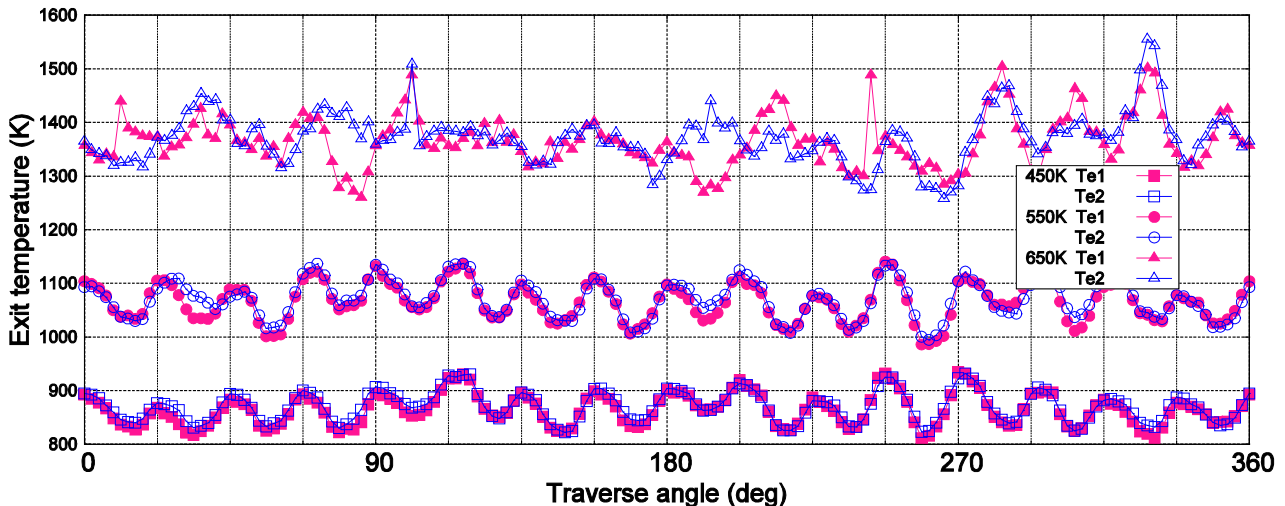


Fig. 12. Circumferential profiles of exit temperature Te1 and Te2 averaged in radial direction.

combustion load got higher, and the shape of the temperature profile became distorted, and the difference between  $Te_1$  and  $Te_2$  also got larger. As the attempt to increase the sampling resolution in the radial direction was based on the assumption of stable combustion, this method was less suitable under 650K condition.

In addition, two-dimensional (in radial and circumferential directions) distributions of the combustor exit temperature  $Te$ , measured by five sampling points on the modified rakes  $Te_1$  and  $Te_2$  and combined to become 10 times 160 sampling points, are shown in Fig.13 for each  $T_{in}$  condition. In these figures, polar plots of radially averaged  $Te_1$  and  $Te_2$  are also shown to be easily compared with the 2D-distributions. For each distribution, the contour color level is selected to enhance the temperature differences. Also from these figures, distributions under 450K and 550K conditions show clear tendency to have peak values between each fuel nozzle, but under 650K condition, this tendency is distorted, especially between 270 and 360 degrees.

In addition, as other indexes to estimate the exit temperature distribution, profiles of Radial Temperature Distribution Factor (R.T.D.F.) and Peak Temperature Factor (P.T.F.) are calculated at each radial span by following equations.

$$R.T.D.F. = \frac{T_{e_{rav}} - T_{e_{av}}}{T_{e_{av}} - T_{in_{av}}}, \quad P.T.F. = \frac{T_{e_{max}} - T_{e_{av}}}{T_{e_{av}} - T_{in_{av}}}$$

Here,  $T_{in}$  and  $Te$  mean combustor inlet and exit temperature, and subscript "av" means radial and circumferential average and "rav" means circumferential average at a radial span. The transition of R.T.D.F. and P.T.F. profiles are shown in Fig.14 for each  $T_{in}$  condition. The lateral axis shows R.T.D.F. and P.T.F., and the vertical axis shows the radial span expressed in percentage terms of the combustor exit height.

As R.T.D.F. is estimated by the average temperature  $Te_{rav}$ , it is not severely affected by the temperature fluctuation, thus the difference between  $Te_1$  and  $Te_2$  profiles is small under all  $T_{in}$ . So, profiles of  $Te_1$  and  $Te_2$  can be combined into smooth lines. On the contrary, as P.T.F. is estimated by the maximum

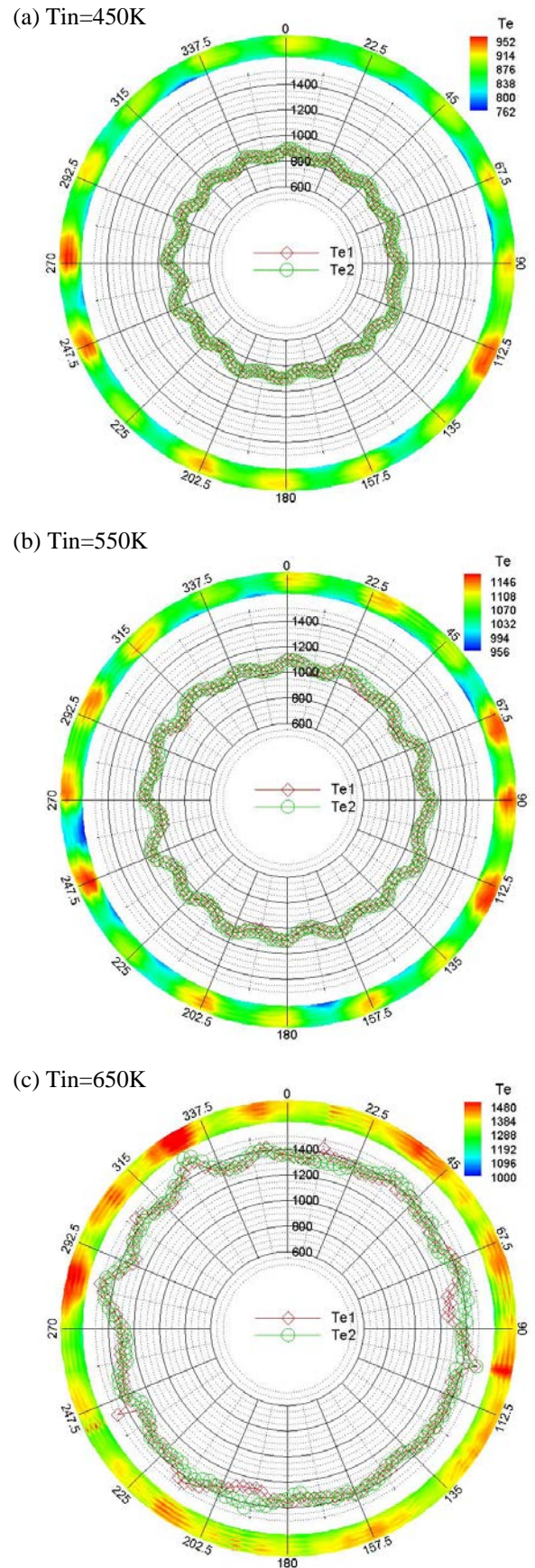


Fig. 13. 2D-distributions of combined exit temperature  $Te$  and circumferential profiles of averaged  $Te_1$  and  $Te_2$ .

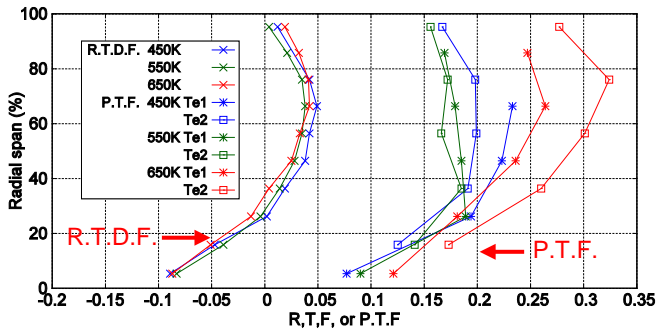


Fig. 14. Radial profiles of R.T.D.F and P.T.F.

temperature  $Te_{max}$ , it is easily affected by the temperature fluctuation, thus the difference between  $Te_1$  and  $Te_2$  profiles is large. So, in Fig.14, profiles of  $Te_1$  and  $Te_2$  are not combined, and plotted separately. Furthermore, the profile of R.T.D.F. was not affected by  $T_{in}$ , but the slopes of P.T.F. got slightly steeper as  $T_{in}$  increased. This means that as the combustion load increased, the fluctuation in the outer region increased and the difference between maximum and average temperature also increased.

### 5 Summary

To investigate the detailed performance of the combustor models, which are developed in the TechCLEAN project of JAXA, combustion tests under parametric conditions were conducted for the rectangular single-sector combustor and the full annular combustor, increasing inlet air temperature from 450K to 700K at intervals of 50K. Even the combustor configuration was different, two combustor models showed similar NOx emission characteristics, but the amount of soot emission was different. For the full annular combustor, detailed traverse measurement at its exit was also conducted, and succeeded to obtain detailed distribution of exit temperature for low load conditions.

### Nomenclature

AFR	Air to Fuel Ratio
CAEP	Committee on Aviation Environmental Protection
EINOx	Emission Index of NOx
ICAO	International Civil Aviation Organization
LTO	Landing and Take-Off

MTO	Max Take-Off
P.T.F.	Peak Temperature Factor
R.T.D.F.	Radial Temperature Distribution Factor
SMD	Sauter Mean Diameter
$T_{in}$	Combustor inlet temperature
$T_e$	Combustor exit temperature
THC	Total Hydrocarbon

### References

- [1] "Aviation and the global atmosphere". *A Special Report of IPCC Working Group I and III*. 1999.
- [2] M. Makida, et al. "Preliminary experimental researches to develop a combustor for small class aircraft engine utilizing primary rich combustion approach". ASME GT2006-91156, 2006.
- [3] M. Makida, et al. "Optimization of a small aircraft combustor to reduce NOx emissions under practical conditions". ASME GT2007-27969, 2007.
- [4] M. Makida, et al. "Verification of low NOx performance of simple primary rich combustion approach by a newly established full annular combustor test facility". ASME GT2008-51419, 2008.
- [5] M. Makida, et al. "Development of Full Annular Combustor for Small Aircraft Jet Engine in JAXA Techclean Project", ICAS2008-559, 2008.
- [6] M. Makida, et al. "Detailed Investigation in Developmental Process of Full Annular Combustor for Small Aircraft Jet Engine", ICAS2010-328, 2010.
- [7] Y. Sugiyama, et al. "Research and development of a 1600°C-level combustor with high heat release rate". ISABE95-7099, 1995.
- [8] Lefebvre, A. H. *Gas turbine combustion, Second edition*. TAYLOR&FANCIS, Philadelphia, 1998.
- [9] Harold C., Simmons et al. "Air-atomizing fuel nozzle". United States Patent, 3980233, Sep.14, 1976.
- [10] W. I. Dodos, et al. "Combustion system design". Chap.4 of *Design of modern turbine combustors*. ACADEMIC PRESS, 1990.
- [11] N. Zarzalis, et al. "NOx-reduction by rich-lean combustion". AIAA PAPER 92-3339, 1992.
- [12] N. K. RIZK and H. C. Mongia. "Three-dimensional NOx modeling for rich/lean combustor". AIAA PAPER 93-0251, 1993.
- [13] Hasegawa, et al. "Effect of pressure on emission characteristics in LBG-fueled 1500C-class gas turbine". ASME 97-GT-277, 1997.
- [14] P. Griebel, et al. "Experimental investigation of an atmospheric rectangular rich quench lean combustor sector for aeroengines". ASME 97-GT-146, 1997.
- [15] J. W. Koopman, et al. "Investigation of a rectangular rich quench lean combustor sector". ASME-98-GT-230, 1998.
- [16] Blomeyer, et al. "Mixing zone optimization of a RQL combustor". *J. of Propulsion and Power*. 15, 2, March/April, pp.288-295, 1999.

## **DETAILED RESEARCH ON RICH-LEAN TYPE SINGLE SECTOR AND FULL ANNULAR COMBUSTOR FOR SMALL AIRCRAFT ENGINE**

- [17] "Procedure for the continuous sampling and measurement of gaseous, emissions from aircraft turbine engines". SAE ARP1256C, 2006.
- [18] Aerospace Recommended Practice. SAE ARP1179, Aircraft Gas Turbine Engine Exhaust Smoke Measurement, rev C 1997.

### **Copyright Statement**

The authors confirm that they, and/or their company or organization, hold copyright on all of the original material included in this paper. The authors also confirm that they have obtained permission, from the copyright holder of any third party material included in this paper, to publish it as part of their paper. The authors confirm that they give permission, or have obtained permission from the copyright holder of this paper, for the publication and distribution of this paper as part of the ICAS 2014 proceedings or as individual off-prints from the proceedings.